

The crystal supramolecularity of metal phenanthroline complexes

Vanessa Russell, Marcia Scudder and Ian Dance *

School of Chemistry, University of New South Wales, Sydney, NSW, 2052, Australia.
E-mail: I.Dance@unsw.edu.au

Received 25th October 2000, Accepted 1st February 2001

First published as an Advance Article on the web 1st March 2001

The 1,10-phenanthroline (phen) ligand in metal complexes commonly forms offset face-to-face (OFF) motifs, and less frequently edge-to-face (EF) motifs. An investigation of the 335 M(phen) complexes, 159 M(phen)₂ complexes, and 33 M(phen)₃ complexes in the Cambridge Structural Database has revealed that in crystals these primary OFF and EF motifs combine to form concerted motifs, and extended motifs, in a variety of ways. Stacks of phen ligands engaging OFF motifs on both faces are very common for complexes M(phen) and M(phen)₂. Even more common for M(phen)₂ are zigzag chains in which each phen ligand links to neighbours in the chain with an OFF motif. The parallel fourfold aryl embrace (P4AE, comprised of one OFF and two EF) occurs for complexes M(phen)₂ and M(phen)₃, with some variety in geometry between a single OFF at one extreme to (EF)₂ at the other. This variability in the P4AE is a consequence of the larger surface area of the phen ligand, compared with those of 2,2'-bipyridyl (bipy) ligands or phenyl groups (which also form this motif), and has been evaluated by calculations of the supramolecular attractive energies. The P4AE associate further, maximising the use of phen surfaces, to form chains of P4AE, chains of P4AE·OFF, and compact two-dimensional nets propagated by both P4AE and OFF motifs. There are examples of three-dimensional nets using these motifs. There is a notable absence of sixfold aryl embraces (6AE, comprised of concerted (EF)₆) amongst M(phen)₃ complexes, and a clear difference with M(bipy)₃ complexes where 6AEs are prevalent. Various M(phen)₂ and M(phen)₃ complexes pack in crystals to form tight hydrophobic domains, often as slabs, segregated from hydrophilic domains containing hydrogen bonding components and anions. The crystallisation and crystal packing of [Co(phen)₃][BF₄]₂·H₂O·EtOH, which exemplifies this pattern, are reported. The implications for crystal engineered enantioselection by [M(phen)₃] complexes are discussed.

Introduction

We have previously described the attractive multiple phenyl embraces between Ph₄P⁺, Ph₃MeP⁺ and MPPH₃ moieties in molecular crystals.^{1–10} These embraces are concerted combinations of the two primary motifs between planar aromatic units, the offset face-to-face (OFF) and edge-to-face (EF) interactions.¹¹ The sixfold phenyl embrace, 6PE, which is the dominant secondary motif between pairs of Ph₄P⁺ cations or PPh₃ units, consists of a concerted cycle of six EF interactions between six phenyl rings. Two other common secondary motifs observed in these systems are the parallel fourfold phenyl embrace (P4PE) and the orthogonal fourfold phenyl embrace (O4PE). Both occur between four phenyl rings, two from each molecule, but are comprised of different combinations of the primary motifs: the P4PE is a composite of one OFF and two EF interactions, and the O4PE is a cycle of four EF interactions. These embraces are not restricted to phenyl substituents. The common ligands 2,2'-bipyridine (bipy) and 2,2' : 6',2''-terpyridine (terpy) present similar faces and edges, and engage in analogous embraces now named multiple aryl embraces. Tris-bipy metal complexes [M(bipy)₃]^z in various oxidation states (*z* = 0, +2 or +3) form sixfold aryl embraces (6AE) at both ends of the molecule along the molecular threefold axis, and thereby infinite chains in crystals.¹² Bis-terpy metal complexes [M(terpy)₂]^z (and also analogous bis(tridentate) metal complexes) show a preference for the P4AE motif, comprised of one OFF and two EF motifs. By use of both faces of the wings of the terpy ligands these P4AE are readily extended into layers, such that two-dimensional nets (called terpy embraces) are prevalent.^{13,14}

We now turn our attention to 1,10-phenanthroline (phen), another planar aromatic ligand occurring frequently in metal

complexes and for which there are many crystal structures and much metric data. Using structures in the Cambridge Structural Database (CSD), and some new crystal structures from our laboratory, we have investigated the crystal supramolecular motifs formed by M–phen complexes. The results, reported here, reveal a large proportion of primary OFF motifs and multiple embraces that contain the OFF motif. These interactions for mono-, bis-, and tris-phen metal complexes can also be extended as nets in one, two and three dimensions. The objectives of this research are to recognise recurring intermolecular motifs, to understand crystal packing in both geometrical and energy terms, and then to apply this knowledge to crystal design and engineering.

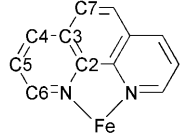
Methodology and experimental

CSD interrogation

The Cambridge Structural Database (CSD, Version 5.18, October, 1999)^{15,16} was interrogated to extract all reliable structures of compounds containing M(phen)_{*n*} where *n* = 1, 2 or 3. Polymetallic complexes containing multiple M(phen)_{*n*} centres are not included in this survey. Searches were then conducted on each of these three sets for the primary motifs OFF and EF, and their combinations.

The search criteria for both the OFF and the EF motif were optimised by analysis of the crystal packing of the resulting hits. The OFF motif consists of two parallel, or close to parallel, ligands which are overlapped. These characteristics were expressed as the following geometrical search parameters: (1) the angle between the normals to two phenanthroline ligand planes be between 0 and 10°; (2) in order to ensure significant overlap, a contact of less than 4 Å exist between the C2 carbon

Table 1 Four charge distributions for [Fe(phen)₃]²⁺ (symmetry *D*₃), and the resulting calculated intermolecular energies for a pair of [Fe(phen)₃]²⁺ cations in representative P4AE geometry



Atom	Set 1	Set 2	Set 3	Set 4
Fe	+0.26	+0.35	+0.41	+0.50
N	−0.20	−0.30	−0.25	−0.32
C2	+0.10	+0.10	+0.10	+0.19
C3	+0.02	+0.05	+0.02	+0.01
C4	−0.07	−0.05	−0.06	−0.09
C5	−0.07	−0.05	−0.06	−0.11
C6	+0.05	+0.05	+0.05	+0.01
C7	−0.06	−0.05	−0.06	−0.12
H4	+0.13	+0.13	+0.13	+0.17
H5	+0.13	+0.13	+0.13	+0.17
H6	+0.12	+0.125	+0.125	+0.16
H7	+0.14	+0.14	+0.14	+0.18
Total energy for P4AE/kcal mol ^{−1}	−8.7	−8.7	−8.8	−9.1
vdW contribution/kcal mol ^{−1}	−17.7	−17.7	−17.7	−17.7
Coulombic contribution/kcal mol ^{−1}	9.0	9.0	8.9	8.6

(see Table 1) of one ligand and a carbon atom of the other ligand; (3) the distance from the centroid of the central C₆ ring of one ligand (see Table 1) to the plane of the other ligand be in the range 3.2–3.6 Å. The search criteria for the EF motif were: (1) the angle between the normals to the phenanthroline ligand planes be allowed to cant 40° either side of perpendicularity, and (2) there be a contact less than 4 Å between any hydrogen atom from one ligand and the centroid of the C₆ ring of the adjacent phenanthroline ligand. This search requires the locations of the hydrogen atoms, but about 30% of the M(phen)_n structures in the CSD do not have deposited hydrogen coordinates: these structures were not analysed in our searches, and this is recognised in the occurrence statistics reported later.

Energy calculations

Our intermolecular potential for atoms *i*, *j* with charges *q_i*, *q_j* separated by *d_{ij}* is eqn. (1), comprising the van der Waals and

$$E_{ij} = e^a_{ij}[(d_{ij}/d^a_{ij})^{-12} - 2(d_{ij}/d^a_{ij})^{-6}] + (q_i q_j)/(\epsilon d_{ij}) \quad (1)$$

coulombic energies. The atom parameters *e^a* (kcal mol^{−1}), *r^a* (Å) are: C, 0.11, 1.95; N, 0.11, 1.95; H, 0.02, 1.68; Fe, 0.15, 2.17. The combination rules are given in eqns. (2) and (3). The

$$d^a_{ij} = r^a_i + r^a_j \quad (2)$$

$$e^a_{ij} = (e^a_i e^a_j)^{0.5} \quad (3)$$

permittivity *ε* in eqn. (1) is distance-dependent, *ε* = 2*d*. Atom partial charges *q* were calculated using the QEq procedure of Rappe and Goddard,¹⁷ as implemented in the MSI Cerius 2 software.¹⁸ This method of equalisation of chemical potential is responsive to geometry. In order to evaluate the effects of different charge distributions we calculated the interaction energies for a pair of [Fe(phen)₃]²⁺ cations in a representative P4AE geometry. The results are presented in Table 1, and indicate that the overall coulombic energy is hardly dependent on the details of charge distribution within chemically reasonable ranges. Charge set 4 was used in all other calculations.

Table 2 Crystal data for complex 1

Formula	C ₃₈ H ₃₂ B ₂ CoF ₈ N ₆ O ₂
<i>M</i>	837.3
Crystal system	Triclinic
Space group	<i>P</i> $\bar{1}$
<i>a</i> /Å	11.309(6)
<i>b</i> /Å	12.926(6)
<i>c</i> /Å	14.429(8)
<i>α</i> /°	81.74(2)
<i>β</i> /°	75.83(3)
<i>γ</i> /°	67.67(3)
<i>V</i> /Å ³	1889(2)
<i>Z</i>	2
<i>μ</i> _{Mo} /mm ^{−1}	0.532
Unique reflections	5255
Observed reflections	3991
<i>R</i> _{merge}	0.011
<i>R</i>	0.055
<i>R</i> _w	0.084

[Co(phen)₃][BF₄]₂·H₂O·EtOH, 1. CoCl₂·6H₂O (3.9 mmol) was dissolved in 35 mL of water and treated with an ethanolic solution of 1,10-phenanthroline (11.6 mmol, in 35 mL). The orange solution produced was heated before treatment with an aqueous solution of NaBF₄ (12.2 mmol in 30 mL). Upon cooling a yellow precipitate formed which was isolated by filtration, washed with water and diethyl ether then dried. Recrystallisation from 25% v/v aqueous ethanol yielded crystals suitable for X-ray analysis.

X-Ray crystallography

Reflection data for complex 1 were measured with an Enraf-Nonius CAD-4 diffractometer in *θ*–2*θ* scan mode using graphite monochromated molybdenum radiation (*λ* 0.7107 Å). Reflections with *I* > 3σ(*I*) were considered observed. The structure was determined by direct phasing and Fourier methods. One of the BF₄[−] anions was disordered over two sites, with major occupancy of 0.737: the BF₄[−] ions were refined as rigid groups with *T_d* symmetry. Phenanthroline ligands were refined with their thermal motion described by 12 parameter TL groups. Reflection weights used were 1/σ²(*F_o*). Atomic scattering factors and anomalous dispersion parameters were from ref. 19. Structure solution was by SIR 92²⁰ and anisotropic refinement used RAELS.²¹ Details of the data collection and refinement are given in Table 2.

CCDC reference number 158795.

See <http://www.rsc.org/suppdata/dt/b0/b008607j/> for crystallographic data in CIF or other electronic format.

Results

The recognised crystal supramolecular motifs involving metal–phenanthroline complexes are described first, progressing from the characteristics of the components, through multiple aryl embraces for pairs of complexes, to extensions in one, two and three dimensions. Calculated motif energies are included with these results. Then the frequency of occurrence of motifs amongst the crystals in the CSD is analysed. In the latter sections some patterns of crystal packing are described, together with the crystal packing of [Co(phen)₃][BF₄]₂·H₂O·EtOH, 1.

Primary motifs: OFF and EF

We first examine the characteristics of the OFF and EF motifs adopted by M(phen)_n complexes. For the OFF a histogram of the distribution of the distance from the C₆ centroid to the adjacent phen plane is shown in Fig. 1. The characteristic of the OFF is a pair of parallel phen ligands, separated by about 3.4 Å. The large surface area means that there can be considerable variation in the degree of overlap of the two rings, while still

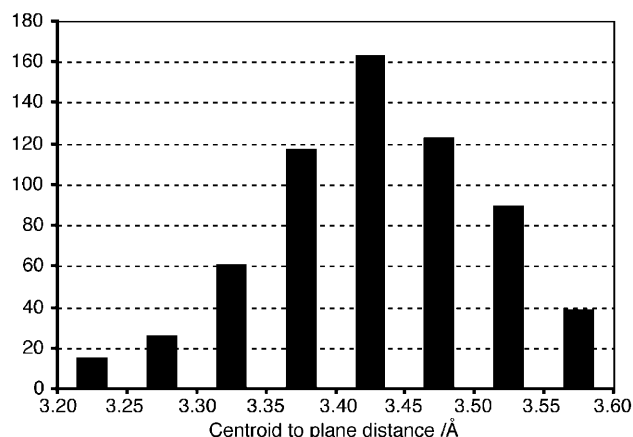


Fig. 1 The distribution of distances between the C_6 centroid and the other phen plane in the OFF primary motif.

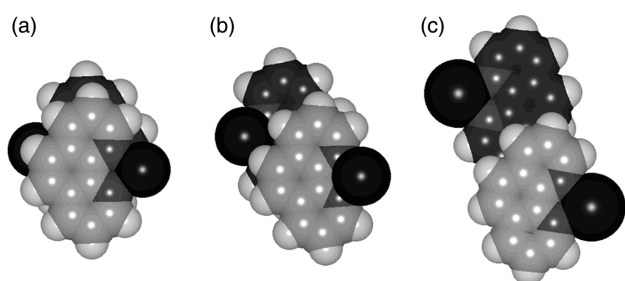


Fig. 2 The range of overlap of phen rings in the OFF motif in crystals: in each picture the C atoms of the lower ring are shaded darker. (a) In BEGCEV (CSD refcode) where there is overlap of all three phen rings. (b) In CATTEW where two rings of each ligand overlap. (c) In VAKROO where only part of one ring of each ligand is overlapped.

adopting a conformation in which the slightly positive H atoms overlay the more negatively polarised carbon atoms. Fig. 2 illustrates the extremes of overlap of the phen ligands in OFF motifs, from a maximum of all three 6-membered rings overlapping (but still offset) to a minimum of half of one such overlapping.

Since the distance between the planes of pairs of rings participating in an OFF interaction is reasonably constant at 3.4 Å, the degree of overlap between phen ligands can be assessed from the distance between the centroids of the ligands. For this purpose the centroid of a phen ligand is defined as the centroid of the central C_6 ring (see Table 1). A centroid-centroid distance < 4 Å represents overlap of three rings (as in Fig. 2(a)), a distance of 4–5 Å is indicative of overlap of two rings (as in Fig. 2(b)), and greater separations indicate lesser overlap. The degree of offset between the phen ligands (the in-plane component of the distance between centroids) can also be calculated, and the distribution of these is presented in Fig. 3. It is clear that there is a wide range of offset, and that the distribution is bimodal around separations of 1–1.5 Å which correspond to the three-ring overlap of Fig. 2(a), and of 3.5–4 Å which represent the two-ring overlap of Fig. 2(b). There are very few structures with an offset < 0.5 Å, corresponding to an eclipsed pairing of the rings, which is electrostatically unfavourable.

The edge-to-face (EF) motif is less prevalent than the OFF interaction. There are three main variables: (1) the angle at which the two rings approach; (2) the section of the phen ligand periphery which provides the edge, and (3) the region of the phen face closest to the approaching edge. The angle between the planes is fairly evenly distributed between 50 and 90° with a slight preference for the higher angles.

Secondary motifs linking pairs of complexes

The primary OFF and EF interactions rarely occur as isolated

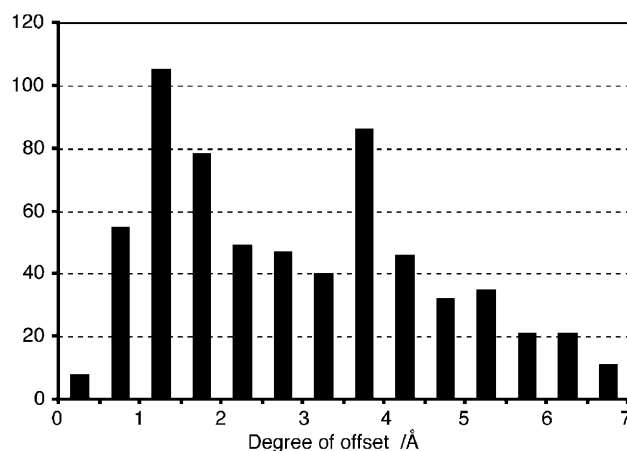


Fig. 3 Histogram of the offset distance (measured in the plane of the ligands) between the centroids of phen ligands in OFF motifs.

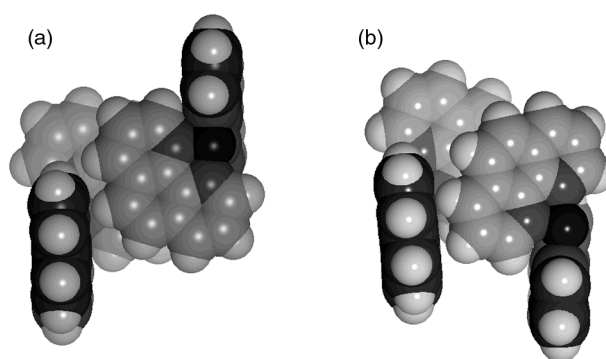


Fig. 4 (a) A typical centrosymmetric P4AE motif between two $M(\text{phen})_2$ moieties of octahedral complexes. The OFF is between the two light coloured phen ligands, and the EF motifs are light to dark. Note that increase of the overlap between the light phen ligands would move their edges away from the faces of the dark ligands. (b) An alternative homochiral $\text{OFF}(\text{EF})_2$ motif which occurs in crystalline $[\text{Mn}(\text{phen})_3]\text{I}_8$,²² shaded as (a) and with the uninvolved phen ligand not shown.

motifs in the crystal lattices of metal-phen complexes. Each phen ligand has two faces and one edge protruding into the crystal environment. The number of possible combinations of primary motifs increases with the number of phen ligands per metal.

The P4AE (parallel fourfold aryl embrace) secondary motif formed between $M(\text{phen})_2$ or $M(\text{phen})_3$ complexes is analogous to that described for phenyl and terpy systems: it requires two phen ligands on each complex, and consists of one OFF and two EF primary motifs, as illustrated in Fig. 4(a).† The P4AE is usually centrosymmetric, and therefore heterochiral. An alternative homochiral motif comprised of OFF plus $(\text{EF})_2$ is also possible: an example, which occurs in the crystal structure of $[\text{Mn}(\text{phen})_3]\text{I}_8$,²² is shown in Fig. 4(b). There is a difference between the P4AE derived from phen ligands and others with phenyl or terpy ligands, which is a consequence of the intramolecular geometry of an octahedral $[M(\text{phen})_2X_2]$ or $[M(\text{phen})_3]$ complex. This is illustrated in Fig. 4(a) for two $M(\text{phen})_2$ moieties of octahedral complexes, showing that favourable overlap of the two phen ligands in the OFF motif moves their edges away from the faces of the other two phen ligands used in the EF motifs. Thus there is conflict between the requirements of the OFF and EF motifs, and the P4AE

† The adjective “parallel” in P4AE refers to the exact or closely parallel relationship between the centroid-M-centroid planes of the two $M(\text{phen})_2$ moieties involved, and originates from the parallel fourfold phenyl embrace where the parallel relationship refers to the $C_{\text{ipso}}\text{-P-}C_{\text{ipso}}$ planes of two Ph_2P moieties.³

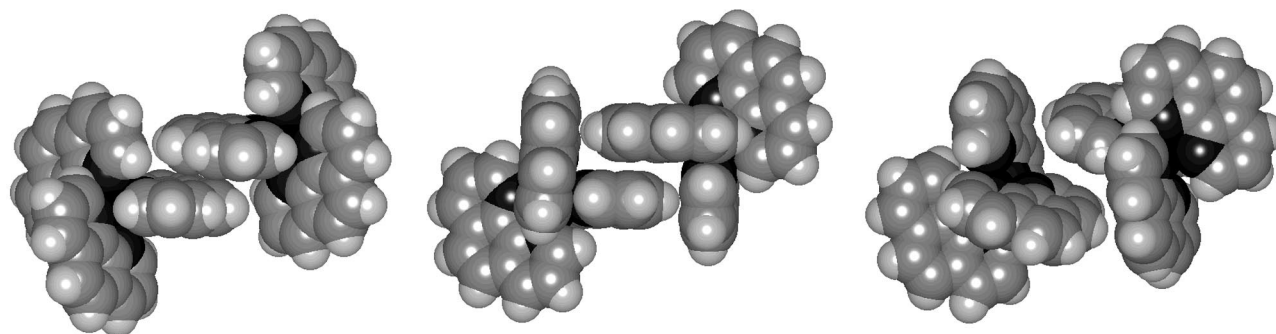


Fig. 5 Examples of the OFF \leftrightarrow P4AE \leftrightarrow (EF)₂ continuum of secondary motifs between M(phen)₃ complexes: (a) OFF in [Ni(phen)₃][Pr⁴OCS₂]₂ [ZELJOP]; (b) P4AE in [Ni(phen)₃][Mn(CO)₅]₂ [PNIMNC10]; (c) (EF)₂ in [Mn(phen)₃][(EtO)₂PS₂]₂ [SOMZOJ].

Table 3 Calculated energies and energy contributions for three structures (see Fig. 5) on the OFF \leftrightarrow P4AE \leftrightarrow (EF)₂ continuum. Atom charges are those of set 4 in Table 1; the vdW and charge parameters for all metals are the same as those for Fe in Table 1; the net charge per phen ligand is +0.5. The total energy is calculated for a pair of complete [M(phen)₃]²⁺ complexes: the sum of the OFF and EF energies does not equal this total because these calculations included only parts of the complex

Calculation	Energy/kcal mol ⁻¹		
	Total	vdW	Coulombic
OFF [ZELJOP]			
Two complete [Ni(phen) ₃] ²⁺	-6.8	-15.5	8.7
OFF phen pair	-9.8	-11.1	1.3
One "EF" phen pair	-0.3	-1.5	1.6
P4AE [PNIMNC10]			
Two complete [Ni(phen) ₃] ²⁺	-9.1	-17.7	8.6
OFF phen pair	-7.2	-7.8	0.7
one EF phen pair	-2.8	-4.0	1.2
(EF)₂ [SOMZOJ]			
Two complete [Mn(phen) ₃] ²⁺	-1.1	-8.9	7.8
"OFF" phen pair	-0.3	-0.8	0.5
one EF phen pair	-2.1	-3.5	1.4

embraces range from those which favour the OFF motif to those which favour the EF motifs. Where the EF primary motifs are poorly developed the secondary motif is effectively just an OFF as already described. At the other extreme of the geometrical range the OFF motif is ineffectual and the secondary motif is essentially a combination of two EF primary motifs. This latter secondary motif is called the double EF interaction, or (EF)₂. There is a continuum of secondary motifs which range from OFF to P4AE to (EF)₂, examples of which are illustrated in Fig. 5.

We have calculated the intermolecular energies for the three motifs shown in Fig. 5, to assess the relative stabilities and contributions to the intermolecular energy for the OFF \leftrightarrow P4AE \leftrightarrow (EF)₂ continuum. The results in Table 3 show that the P4AE motif has the most favourable attractive energy of *ca.* 9 kcal mol⁻¹ per {[M(phen)₃]²⁺}₂, comprised of 17.7 kcal mol⁻¹ attractive van der Waals (vdW) energy and 8.6 kcal mol⁻¹ net Coulombic repulsion. In the P4AE the OFF motif contributes more attraction (7.2 kcal mol⁻¹) than the pair of EF motifs (2 × 2.8 kcal mol⁻¹). The primarily OFF motif of [Ni(phen)₃]-[Pr⁴OCS₂]₂ [refcode ZELJOP] in Fig. 5(a) similarly has a net attraction of 6.8 kcal mol⁻¹, of which the OFF pair of phen ligands contribute 9.8 kcal mol⁻¹ attraction. The (EF)₂ motif in [Mn(phen)₃][(EtO)₂PS₂]₂ [SOMZOJ] (Fig. 5(c)) is only weakly attractive.

Some of the variability of P4AE motifs has been illustrated in the dimorphs of the five-coordinate complex [Cu(phen)₂]⁺ as I₃⁻ salt.²³ In these dimorphs there is a substantial difference

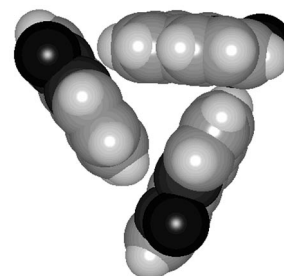


Fig. 6 The (EF)₃ interaction in [{Cu(phen)(PPh₂)}₃] [NAWMUT]: only Cu(phen) is shown for each of the three interacting molecules.

in the angle between the planes of the two phen ligands, but in both cases there are well developed P4AE secondary motifs. The overall crystal packing is similar in these dimorphs, and involves further associations of the two different P4AE motifs.

It is also possible for M(phen) complexes to associate with three EF interactions between them, (EF)₃. An example is shown in Fig. 6 for the cyclic trimer [{Cu(phen)(PPh₂)}₃] [NAWMUT] where there is a cycle of EF interactions between three ligands.

The 6AE secondary motif is extremely rare in [M(phen)₃] complexes. We know of two polyiodide compounds which include this motif, [Fe(phen)₃]₂I₈²² and [Mn(phen)₃]₂I₃₂.²⁴ The rarity is believed to be due to the less competitive attractive energy of the EF motif *versus* OFF for phen ligands: the 6AE contains only EF and no OFF primary motifs. The occurrence of 6AE in polyiodide salts of [M(phen)₃]²⁺ is related to the close association of the polyiodide chains with the exposed grooves between the phen ligands.²⁵

Extended motifs

The OFF stack. Each phen ligand possesses two faces, both of which are capable of participating in OFF interactions with neighbouring ligands. The offset stacking of phen ligands to maximise this favourable OFF motif is common, and is named the OFF stack. An example is shown in Fig. 7. The stack is usually infinite, with the M atoms alternating on either side of the stack. As illustrated in Fig. 7 the stack can be reinforced by hydrogen bonds or interactions on the edges. The OFF stack is common in M(phen), M(phen)₂, and M(phen)₃ complexes, and as described below, can combine with other phen motifs.

OFF zigzag chains. The OFF chain motif occurs commonly in bis- and tris-phen complexes, which are linked into chains using two phen ligands and two separate OFF motifs with adjacent complexes. The most common type of OFF chain is that illustrated in Fig. 8. In each complex the outer faces of the two phen ligands overlap the corresponding faces of neighbouring molecules. We note that the example of the OFF zigzag chain shown is one of the [Fe(phen)₂(NCS)₂] compounds which demonstrates anomalous spin-state transitions in the crystal-

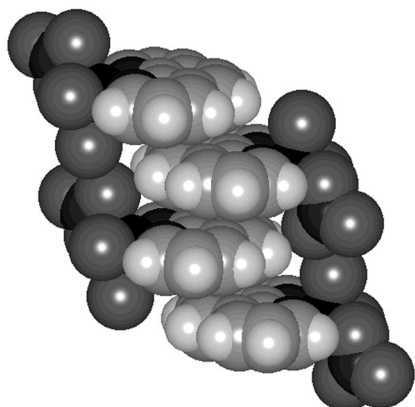


Fig. 7 OFF stack motif in $[\text{Cu}(\text{phen})(\text{NO}_3)(\text{H}_2\text{O})_2]\text{NO}_3$ [ANPNCU]. In this example, hydrogen bonds between nitrate and water molecules on the edges reinforce the stack.

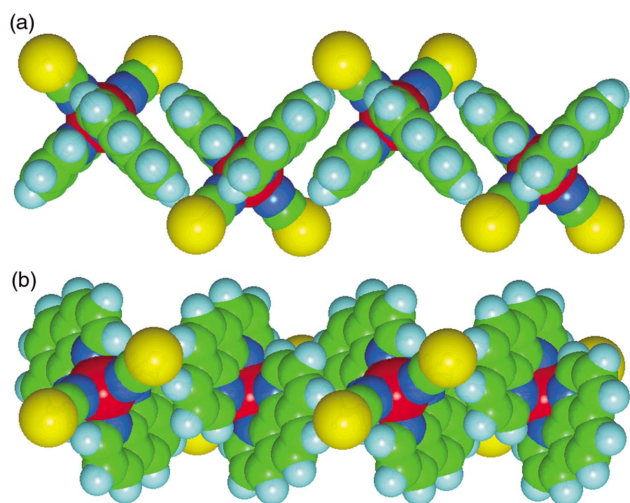


Fig. 8 The OFF zigzag chain, as occurs in $[\text{Fe}(\text{phen})_2(\text{NCS})_2]$ [KEKVIF]: Fe, red; C, green; N, dark blue; S, yellow; H, pale blue. (a) Side view showing the OFF motifs using the outer surfaces of the phen ligands. (b) Top view, showing the overlap of one pyridyl ring in each phen ligand.

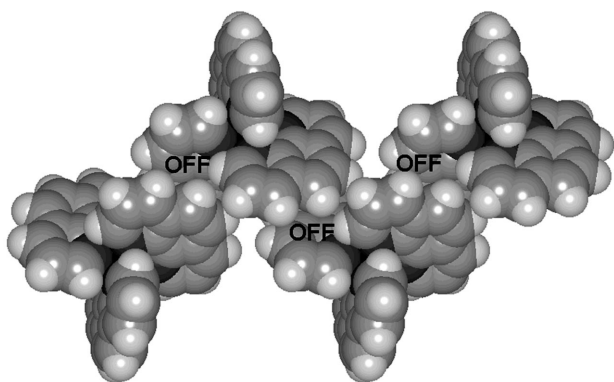


Fig. 9 The inner OFF chain as it occurs in $[\text{Fe}(\text{phen})_3][\text{I}_3]_2 \cdot \text{CH}_2\text{Cl}_2$.³¹ OFF motifs are formed between pairs of phen ligands which are all parallel to the axis of the chain.

line state.^{26,27} Structural changes accompany continuous and discontinuous spin-state transitions, and the crystal supramolecularity of these compounds is relevant to the physical properties.^{28–30}

There is an alternative form of the OFF zigzag chain motif, shown in Fig. 9 as it occurs in $[\text{Fe}(\text{phen})_3][\text{I}_3]_2 \cdot \text{CH}_2\text{Cl}_2$,³¹ and differing in two respects from that shown in Fig. 8. One difference is that the surfaces of the phen ligands involved in the OFF motifs are the inner faces relative to the cleft between

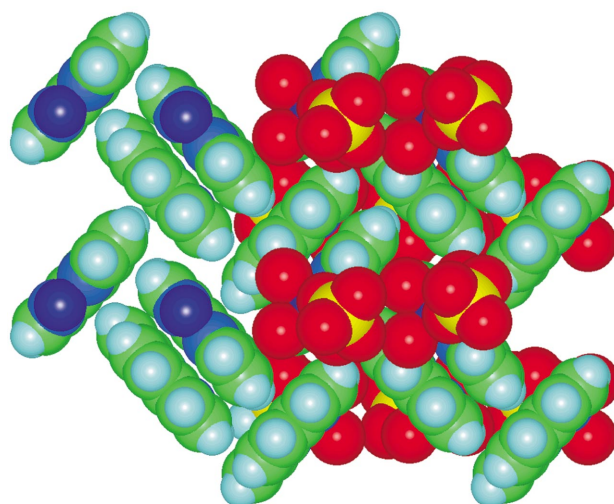


Fig. 10 The herringbone array of phen ligands in OFF pairs in $[\text{Co}(\text{phen})(\text{SO}_4)(\text{H}_2\text{O})_3]$ [FICNOU]. On the left side of the figure the sulfate and water ligands have been omitted to reveal the phen array.

ligands, as opposed to the outer faces used in Fig. 8. Accordingly, the more common motif shown in Fig. 8 is named the outer OFF chain, and that of Fig. 9 is named the inner OFF chain. The other difference between these is in the relationship between the direction of propagation of the chain and the direction of the phen planes involved. In the outer OFF chain (Fig. 8) the cleft between the phen planes is perpendicular to the propagation axis, while in the inner OFF chain (Fig. 9) the phen cleft is parallel to the propagation axis.

Two-dimensional net of OFF and EF

In the crystal structure of the mono-phen complex $[\text{Co}(\text{phen})(\text{SO}_4)(\text{H}_2\text{O})_3]$ [FICNOU] the phen ligands are aligned perpendicular to a layer, in herringbone array. This is illustrated in Fig. 10. The close-packed array of phen ligands is actually a herringbone arrangement of $(\text{phen})_2$ in OFF motif. Each OFF $(\text{phen})_2$ pair functions as EF donor to two other such pairs, and EF acceptor to two more such pairs. This packing feature is closely analogous to the packing of polycyclic aromatic hydrocarbons, and is in fact the type labelled as “sandwich herringbone” by Desiraju and Gavezzotti³² in their classification and analysis of the crystal packing of polycyclic aromatic hydrocarbons. The hydrocarbon phenanthrene, related to the phen ligand, crystallises with the simple herringbone structure as occurs in crystalline benzene, not with the sandwich herringbone structure of FICNOU.

P4AE·OFF chains and layers

The P4AE motif for $\text{M}(\text{phen})_2$ has four exterior phen surfaces, two belonging to ligands involved in the OFF of the P4AE, and two from the ligands accepting the EF interactions. These four external faces of the P4AE motif form an approximately rectangular box, and both types of outer surface are available for interaction, *via* further OFF motifs, with other P4AE motifs. This leads to extension of the motifs in one or two dimensions. Fig. 11 shows the repetition of P4AE motifs by formation of an OFF outside each of the phen ligands of the P4AE, as occurs in crystalline $[\text{Tc}(\text{N})(\text{phen})_2\text{Cl}]\text{PF}_6$ [KUKHIH]: this motif is $\cdot\text{P4AE}\cdot\text{OFF}\cdot\text{P4AE}\cdot\text{OFF}\cdot$. Fig. 12 shows a two-dimensional net generated by extension at all four external faces of a P4AE, as occurs in $[\text{Zn}(\text{phen})_2(\text{H}_2\text{O})_2]\text{SO}_4 \cdot 6\text{H}_2\text{O}$ [KOFCUD]. The repetition is $\cdot\text{P4AE}\cdot\text{OFF}\cdot\text{P4AE}\cdot\text{OFF}\cdot$ in both directions, forming a compact layer of phen ligands. Within the layer each phen ligand is involved in two local motifs, either $\{2 \times \text{OFF} + \text{EF}\}$ or $\{\text{OFF} + \text{EF}\}$. One of the water ligands at Zn is retained within the layer, while the other is directed towards the interlayer space, which contains the

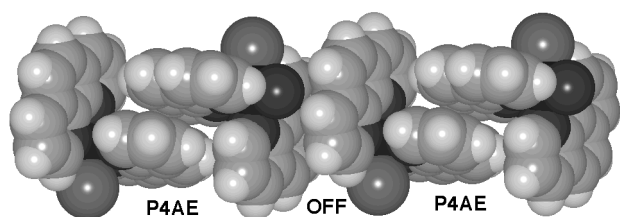


Fig. 11 Part of the $\cdot\text{P4AE}\cdot\text{OFF}\cdot\text{P4AE}\cdot\text{OFF}\cdot$ chain in $[\text{Tc}(\text{N})(\text{phen})_2\text{-Cl}]\text{PF}_6$ [KUKHIH].

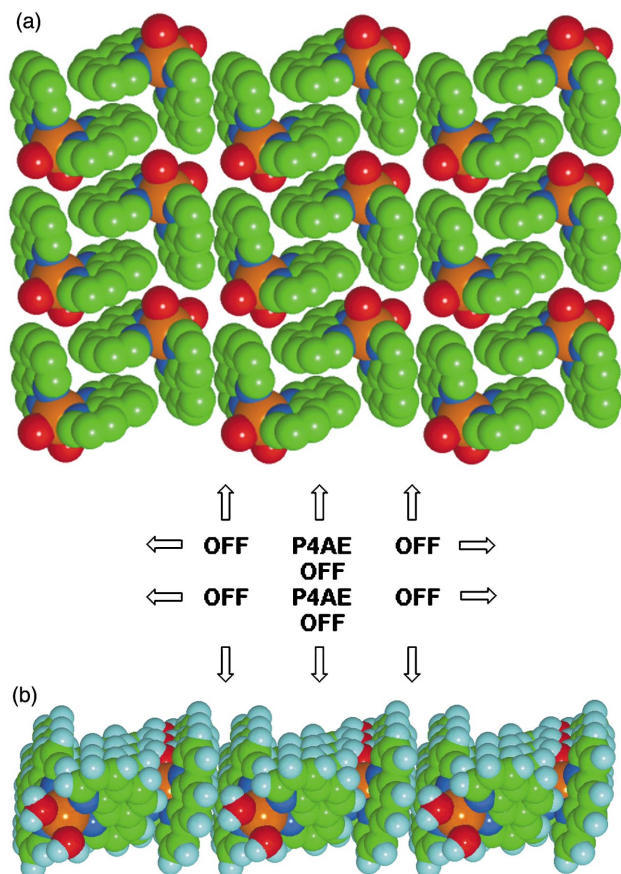


Fig. 12 Two views of the layered crystal structure of $[\text{Zn}(\text{phen})_2(\text{H}_2\text{O})_2]\text{SO}_4\cdot 6\text{H}_2\text{O}$ [KOFUD]. (a) Normal to the layer, showing the compact array of P4AE and OFF motifs; Zn, orange; H atoms not shown. (b) View almost perpendicular to the layer.

SO_4^{2-} ions and other water molecules in a layer of hydrogen bonds. This crystal is an excellent example of layered segregation of hydrophobic and hydrophilic domains (Fig. 12).

The structure of $[\text{V}(\text{phen})_2(\text{O}_2)\text{O}]\text{ClO}_4$ [JAMCUV10] is a two-dimensional array, similar to the preceding, but without P4AE motifs (see Fig. 13). For a P4AE to exist the second ligand on each of the pair of interacting $\text{M}(\text{phen})_2$ moieties must be oriented in opposing directions, to allow for formation of the pair of EF interactions. In JAMCUV10, however, all these ligands point in the same direction (upwards for the OFF stacks to the left and right of Fig. 13 and downwards for the stack in the centre). In place of the P4AE interactions there are further EF interactions.

P4AE chains and nets

The foregoing chains and layers of P4AE and OFF motifs are not possible for $\text{M}(\text{phen})_3$ complexes with octahedral coordination because the third phen ligand interferes. Instead, $\text{M}(\text{phen})_3$ complexes form multiple P4AE motifs, using two or three of the $\text{M}(\text{phen})_2$ clefts apparent when the molecule is viewed down its (real or pseudo) threefold axis. A chain of

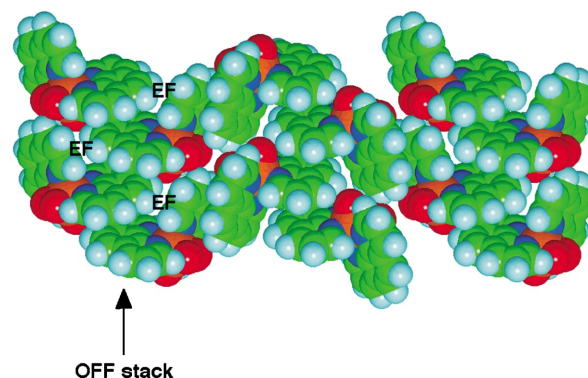


Fig. 13 The two-dimensional array formed by $[\text{V}(\text{phen})_2(\text{O}_2)\text{O}]\text{ClO}_4$ [JAMCUV10]. There is a combination of OFF stacks and chains, and EF motifs, but no P4AE.

P4AE can form, using two of the clefts: alternate P4AEs along the chain are rotated by 90° . This P4AE chain motif has been recognised previously in polyiodides of $[\text{Fe}(\text{phen})_3]^{2+}$.³³ If the three clefts of $\text{M}(\text{phen})_3$ are used for P4AE motifs a two-dimensional net can be formed, and a crystal structure which demonstrates this is $[\text{Cu}(\text{phen})_3][\text{O}_3\text{SSSO}_3]\cdot 5\text{H}_2\text{O}$ [NILTEH], shown in Fig. 14. Within the well defined layer structure there are zigzag chains of P4AE motifs, further connected by P4AE motifs, to yield a hexagonal net of P4AE (Fig. 14(a)). This layer is a very compact packing of phen ligands. Fig. 14(b), a slightly different view of the layer, shows that there are regions (in the centres of the hexagons of Fig. 14(a)) where four phen ligands from four different $[\text{Cu}(\text{phen})_3]$ complexes come together in a box motif, and that propagation of this yields a domain which is similar to the terpy layer embrace shown in Fig. 14(c). Differences between this phen box and the terpy layer are the stepped nature of the phen box, and its OFF which is absent in the terpy embrace. The third phen ligand of $\text{M}(\text{phen})_3$ is orthogonal to the axis of the phen box, and therefore blocks any nascent terpy embrace with stepped ribbons of phen in OFF local motif: two such ribbons are present in Fig. 14(b). Stepped layers of $[\text{Cu}(\text{phen})_3]^{2+}$ in NILTEH are separated by layers of tetrathionate anions $[\text{O}_3\text{SSSO}_3]^{2-}$ and water molecules, linked by hydrogen bonds. The crystal structure of NILTEH is another excellent example of clear segregation of strongly hydrophobic and strongly hydrophilic domains.

Three-dimensional nets

Since $[\text{M}(\text{phen})_3]$ complexes can form compact two-dimensional nets constructed from OFF and P4AE motifs, the question arises as to whether three-dimensional nets are possible. We describe here one example, in crystalline $[\text{Mn}(\text{phen})_3]\text{-}[\text{S2P}(\text{OEt})_2]$ [SOMZOJ], in which each $[\text{Mn}(\text{phen})_3]^{2+}$ cation is linked to four neighbouring cations *via* two OFF primary interactions and two $(\text{EF})_2$ motifs, illustrated in Fig. 15(a). These supramolecular linkages around each cation are approximately tetrahedral, and when propagated through the lattice generate the diamondoid net shown in Fig. 15(b).

Frequencies of occurrence of motifs

We have generated statistics on the frequencies of occurrence of the major features described above. Frequencies of occurrence reflect relative stabilities. It is not always possible to be exact, due to variations in motif geometry and the requirement for manual searches in some cases, but we believe that the figures presented in Table 4 provide good account of occurrences in the CSD. The analyses for EF motifs in the $\text{M}(\text{phen})$ and $\text{M}(\text{phen})_2$ sets were restricted to structures for which hydrogen atom coordinates are deposited in the CSD. The principal result (Table 4) is the frequent occurrence of OFF motifs for M–phen complexes. OFF motifs occur in 70% of $\text{M}(\text{phen})$ crystals, 84%

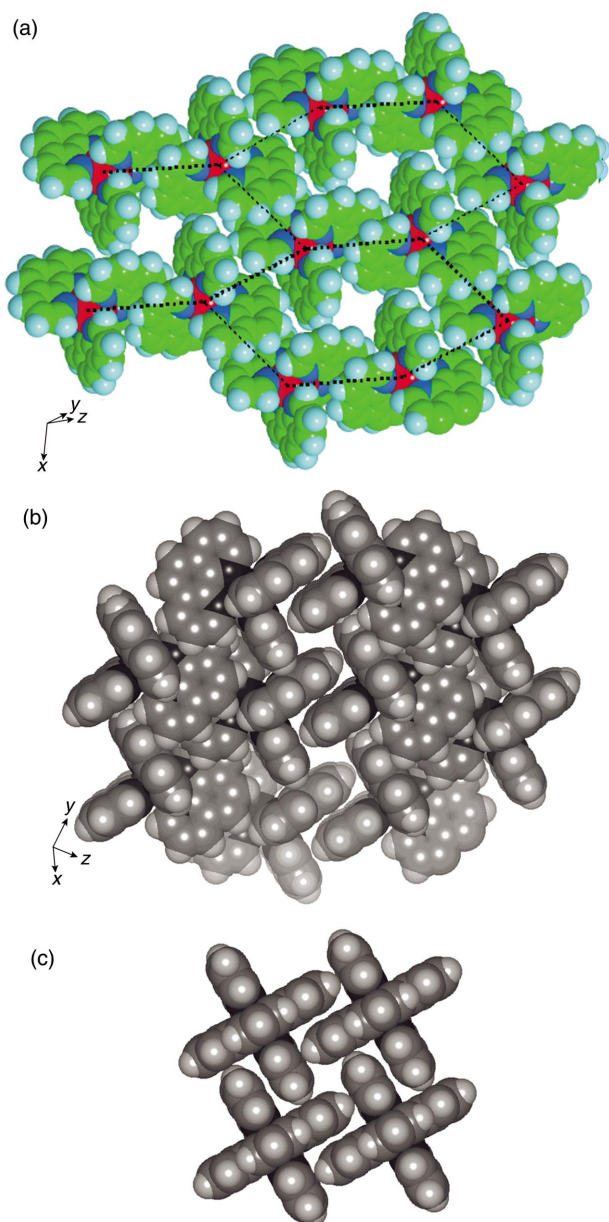


Fig. 14 Part of the crystal structure of $[\text{Cu}(\text{phen})_3][\text{O}_3\text{SSSO}_3]\cdot 5\text{H}_2\text{O}$ [NILTEH]. (a) View normal to the layer of $[\text{Cu}(\text{phen})_3]^{2+}$ ions which are fully engaged in P4AE motifs, which form a hexagonal net: each broken line represents a P4AE. (b) View of the layer which shows different aspects of the P4AEs, namely the phen-box motifs on the centre line, and two stepped ribbons of phen rings in OFF motifs. (c) Axial view of part of the terpy embrace two-dimensional net,¹³ showing the similarity and difference with the central region of the NILTEH net in (b).

of $\text{M}(\text{phen})_2$ crystals, and 61% of $\text{M}(\text{phen})_3$ crystals. It can be concluded that it is unusual for an $\text{M}(\text{phen})_n$ complex (for $n = 1, 2$ or 3) not to participate in an OFF motif. In contrast, the EF motif is much less common, occurring in <3% of $\text{M}(\text{phen})$ crystals and 40% of $\text{M}(\text{phen})_2$ crystals: the molecular geometry of the $\text{M}(\text{phen})_3$ complexes tends to enforce EF motifs, and they are found in 76% of these crystals.

The P4AE motif has been detected in 16% of the crystals of $\text{M}(\text{phen})_2$ compounds and 36% of the crystals of $\text{M}(\text{phen})_3$ compounds in the CSD. A considerable number of the crystal structures of $\text{M}(\text{phen})_2$ and $\text{M}(\text{phen})_3$ compounds recently determined in our laboratories contain the P4AE motif.^{23,25,33,34}

Patterns of crystal packing for $[\text{M}(\text{phen})_3]$ complexes

Having recognised recurring supramolecular motifs, the next stage in understanding the crystal supramolecularity of M-phen complexes is analysis of their complete crystal

Table 4 Statistics for occurrence of $\text{M}(\text{phen})_n$ complexes in the CSD and the number of structures demonstrating the various supra-molecular motifs^a

	$\text{M}(\text{phen})$	$\text{M}(\text{phen})_2$	$\text{M}(\text{phen})_3$
Number of compounds in the CSD	335	159	33
Number of compounds with H coordinates	238	112	23
OFF primary motifs	233	134	20
EF primary motifs	6 ^b	45 ^b	25
P4AE motifs	—	25	12
(EF) ₂ motifs	—	25 ^b	6
6AE motifs	—	—	0 ^c
OFF stacks	99	43	7
OFF chains	—	107	12

^a A dash indicates that the category is not applicable. ^b The search for this motif was made only on the structures for which hydrogen coordinates are included in the CSD. ^c We are aware of two instances not yet in the CSD.

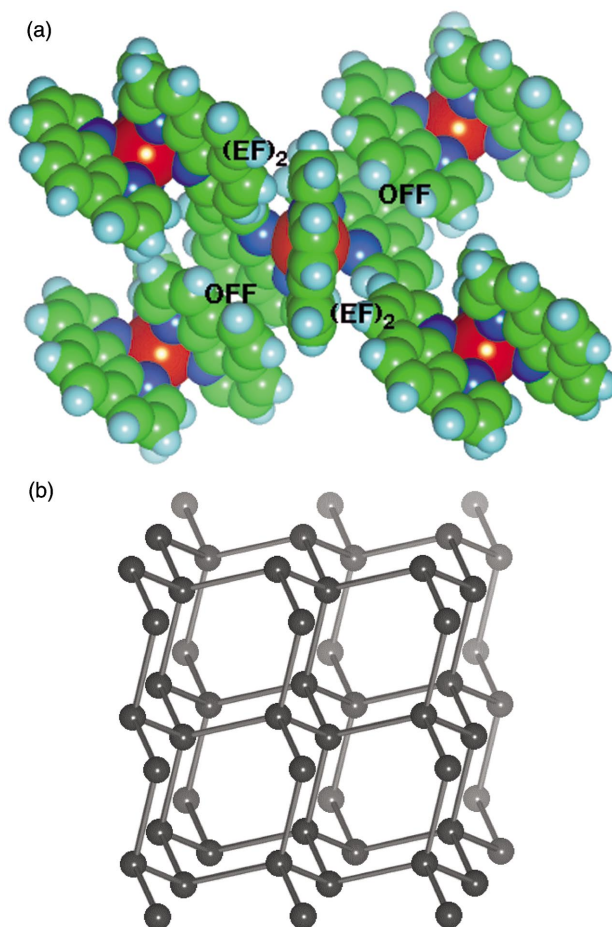


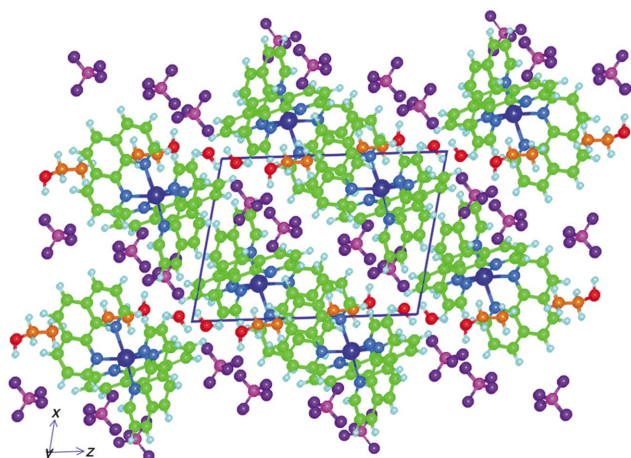
Fig. 15 Representations of the crystal structure of $[\text{Mn}(\text{phen})_3][\text{S}_2\text{P}(\text{OEt})_2]$ [SOMZOJ]. (a) Four $[\text{Mn}(\text{phen})_3]^{2+}$ ions surrounding one, with OFF and (EF)₂ supramolecular connections: see also Fig. 5(c): Mn, orange. (b) The diamondoid net generated by the pseudo-tetrahedral supramolecular connections to each $[\text{Mn}(\text{phen})_3]^{2+}$: Mn, black.

packings, which manifest the outcomes of the competitions and synergies of possible motifs. We present here an analysis of crystal packing in some $[\text{M}(\text{phen})_3]^{2+,3+}$ complexes with relatively simple anions, and identify some patterns.

Table 5 contains crystallographic information for $[\text{M}(\text{phen})_3]^{2+,3+}$ complexes crystallised with the small symmetrical anions NO_3^- , BF_4^- , ClO_4^- and PF_6^- . One of these, $[\text{Co}(\text{phen})_3][\text{BF}_4]_2\cdot \text{H}_2\text{O}\cdot \text{EtOH}$, **1**, is reported here, while the others are from the CSD. Six crystals containing $[\text{M}(\text{phen})_3]^{2+}$

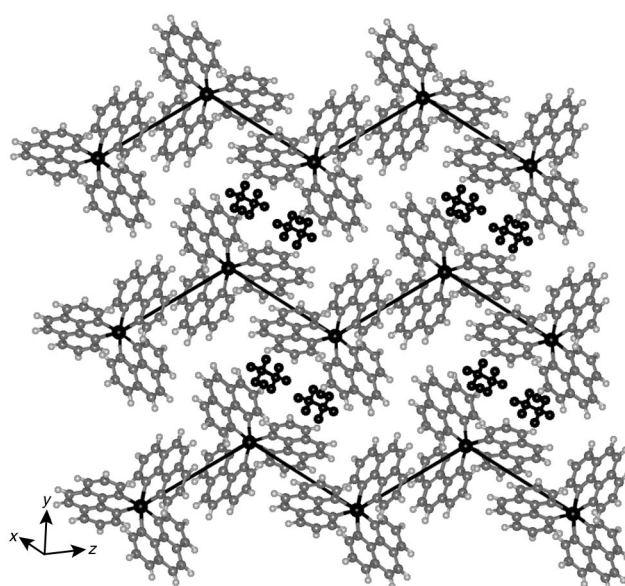
Table 5 Crystals of compounds containing $[\text{M}(\text{phen})_3]^{2+,3+}$ with small anions

REFCODE	Compound	Space Group	Relevant cell dimensions in Å; °
This work	$[\text{Co}(\text{phen})_3][\text{BF}_4]_2 \cdot \text{H}_2\text{O} \cdot \text{EtOH}$, 1	$P\bar{1}$	11.3, 12.9, 14.4; 81.7, 75.8, 67.7
DAWLES	$[\text{Os}(\text{phen})_3][\text{ClO}_4]_2 \cdot \text{H}_2\text{O}$	$C2/c$	35.9, 16.0, 12.4; 102.4
PENCUC	$[\text{Cu}(\text{phen})_3][\text{ClO}_4]_2$	$C2/c$	36.0, 16.0, 12.2; 101.7
QQQBES01	$[\text{Co}(\text{phen})_3][\text{ClO}_4]_2 \cdot \text{H}_2\text{O}$	$C2/c$	36.4, 15.9, 12.3; 102.8
WERLIO	$[\text{Fe}(\text{phen})_3][\text{ClO}_4]_2 \cdot 0.5\text{H}_2\text{O}$	$C2/c$	36.4, 15.9, 12.1; 102.1
TEVHIL	$[\text{Ni}(\text{phen})_3][\text{ClO}_4]_2 \cdot 0.5\text{H}_2\text{O}$	$C2/c$	36.7, 15.7, 12.3; 102.9
ZUZSIW	$[\text{Ru}(\text{phen})_3][\text{PF}_6]_2$	$C2/c$	37.1, 16.0, 12.1; 101.4
TUMVOM	$[\text{Ni}(\text{phen})_3][\text{NO}_3]_2 \cdot \text{CHCl}_3 \cdot \text{H}_2\text{O}$	$P2_1/c$	17.0, 12.3, 20.3; 108.3
RUGTIW	$[\text{Cd}(\text{phen})_3][\text{ClO}_4]_2 \cdot 2\text{H}_2\text{NC}_6\text{H}_4\text{NO}_2 \cdot p$	$C2/c$	25.1, 10.8, 19.4; 116.6
RAVJIH	$\Lambda\text{-}[\text{Ru}(\text{phen})_3][\text{PF}_6]_2 \cdot \text{CH}_3\text{CN} \cdot \text{EtOEt}$	$P4_3 (Z = 2)$	25.4, 12.7
OPENFE	$[\text{Fe}^{\text{III}}(\text{phen})_3][\text{ClO}_4]_3 \cdot 2\text{H}_2\text{O}$	$A2/a$	23.3, 18.3, 17.8; 92.5
QQQBEV01	$[\text{Co}^{\text{III}}(\text{phen})_3][\text{ClO}_4]_3 \cdot 2\text{H}_2\text{O}$	$C2/c$	17.8, 18.3, 23.1; 92.7

**Fig. 16** The crystal lattice of $[\text{Co}(\text{phen})_3][\text{BF}_4]_2 \cdot \text{H}_2\text{O} \cdot \text{EtOH}$, **1**. The slabs of $[\text{Co}(\text{phen})_3]^{2+}$ cations run top left to bottom right, separated by the BF_4^- ions (B, pink; F, purple) and water (O, red). The ethanol molecules (C, orange) can be seen to have their alkyl chains embedded in the cation layer while their hydroxy groups protrude into the anions/solvent layer.

with ClO_4^- or PF_6^- are isomorphous in space group $C2/c$, and contain 0, 0.5 or 1 H_2O per formula unit, while $[\text{Co}(\text{phen})_3][\text{BF}_4]_2 \cdot \text{H}_2\text{O} \cdot \text{EtOH}$ **1** crystallises in $P\bar{1}$. We therefore describe the crystal packing in each of these types, seeking to understand the minor difference.

The crystal lattice of complex **1** contains slabs of $[\text{Co}(\text{phen})_3]^{2+}$ cations alternating with hydrogen bonded anions and solvent molecules (Fig. 16). Within the slabs of cations the principal motif is the extended P4AE chain, in which each $[\text{Co}(\text{phen})_3]^{2+}$ participates in two slightly different P4AE alternating along each chain. As shown in Fig. 17 the zigzag P4AE chains are aligned side by side to generate the slab of $[\text{Co}(\text{phen})_3]^{2+}$. Between these chains there are no standard aryl embraces, but instead aryl boxes that are generated by four phen ligands from two $[\text{Co}(\text{phen})_3]^{2+}$ complexes around a centre of inversion. Each box houses two ethanol molecules. The ethyl chains reside within the hydrophobic box, while the OH groups protrude from the box and participate in hydrogen bonding with the water molecules in the adjacent layers. Fig. 18 shows details of the aryl box and its filling with ethanol. The ethanol OH, water, and BF_4^- ions (one of which is orientationally disordered) occur on the edge of the slab of cations, and participate in $\text{BF}_4^- \cdots \text{HO}(\text{Et}) \cdots \text{HOH} \cdots \text{F}_4\text{B}^-$ hydrogen bonds. Our full interpretation of the crystal supramolecularity of **1** therefore postulates P4AE as the principal motif, with the formation of fully hydrophobic slabs within the crystal. The counter anions, BF_4^- , occupy the inter-slab spaces, but having relatively small volume allow hydrogen bonding solvent also to occupy these hydrophilic domains. By crystallising with one water molecule and one ethanol molecule hydrogen bound in this domain, the ethyl chains are able to form the known filled

**Fig. 17** The layer of parallel zigzag P4AE chains in $[\text{Co}(\text{phen})_3][\text{BF}_4]_2 \cdot \text{H}_2\text{O} \cdot \text{EtOH}$, **1**. The P4AE motifs are indicated by $\text{Co} \cdots \text{Co}$ rods. The ethanol molecules and water oxygen atoms are black, and indicate the positions of the filled aryl box motifs formed between the P4AE chains.

aryl box (FAB) motif^{22,35} between the zigzag P4AE chains in the hydrophobic slab.

The crystal packing in one instance ($[\text{Os}(\text{phen})_3][\text{ClO}_4]_2 \cdot \text{H}_2\text{O}$ [DAWLES]) of the related compounds in the $C2/c$ lattice structure type (Table 5) is shown in Fig. 19. Again there are segregated hydrophobic and hydrophilic slabs, the latter containing the ClO_4^- and H_2O . The $[\text{Os}(\text{phen})_3]^{2+}$ complexes are associated in chains of P4AE, but with a variation of the local P4AE geometry such that there is an OFF stack of phen ligands also propagated along the P4AE chain axis. This is shown in Fig. 20, to be compared with Fig. 17. This one-dimensional motif is therefore a combination of the OFF stack and the zigzag P4AE chain described above. The fact that this occurs in a number of isostructural crystals with slightly different compositions implies appreciable stability. Adjacent P4AE chains are linked *via* OFF interactions (Fig. 20).

There are clearly similarities between the local interactions taking place in this structure type and that described above for complex **1**, with chains of cations linked by P4AE present in both. A subtle but possibly significant difference between **1** and the $C2/c$ structure type is the presence of ethanol in the lattice of **1**, and the formation of the filled aryl box. A question that arises is whether this filled aryl box is a causative or derivative motif. The crystallisations of three [QQQBES01, RUGTIW, QQQBEV01] of the eight “ $C2/c$ compounds” in Table 5 were in the presence of ethanol, and so there was unfulfilled opportunity to form the FAB motif.

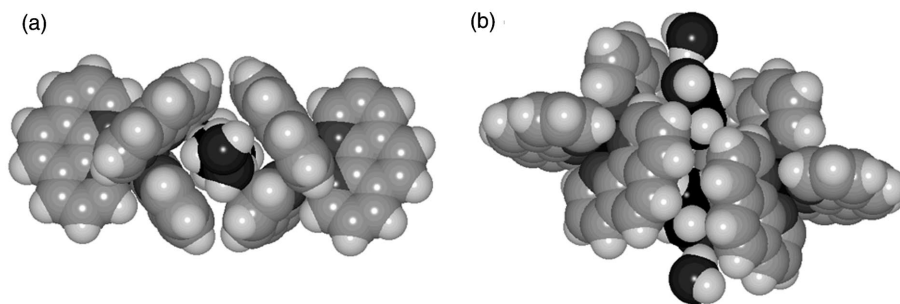


Fig. 18 (a) The inclusion of solvent ethanol in the aryl box constructed from four phen ligands. (b) The view normal to (a). Where the hydroxy groups protrude from the ends of the box they take part in hydrogen bonding to solvent water.

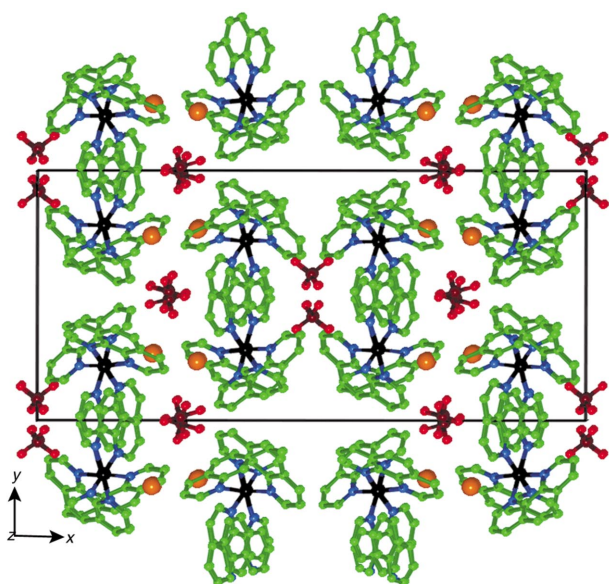


Fig. 19 The crystal packing in $[\text{Os}(\text{phen})_3][\text{ClO}_4]_2 \cdot \text{H}_2\text{O}$ [DAWLES]: Os, black; C, green; Cl, brown; O (ClO_4^-), red; O (H_2O), orange; space group $C2/c$. The hydrophobic layers comprised only of embracing $[\text{Os}(\text{phen})_3]^{2+}$ complexes are parallel to the yz plane, separated by domains containing the ClO_4^- and H_2O .

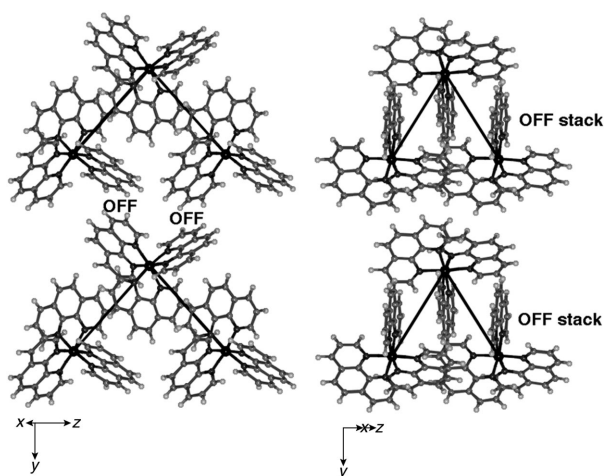


Fig. 20 Two views of the slab of embracing $[\text{Os}(\text{phen})_3]^{2+}$ complexes in crystalline $[\text{Os}(\text{phen})_3][\text{ClO}_4]_2 \cdot \text{H}_2\text{O}$ [DAWLES]. P4AE linkages are marked by $\text{Os} \cdots \text{Os}$ rods. The left view, perpendicular to the slab, shows how adjacent zigzag P4AE chains are linked by OFF motifs. Rotation of this section about the y axis yields the picture on the right, which shows how there is a stack of OFF motifs between phen ligands along each P4AE chain.

Crystal packing for single enantiomers of $[\text{M}(\text{phen})_3]$ complexes

All of the above compounds are racemic, and crystallised in centrosymmetric lattices. Resolved $[\text{M}(\text{phen})_3]$ complexes could

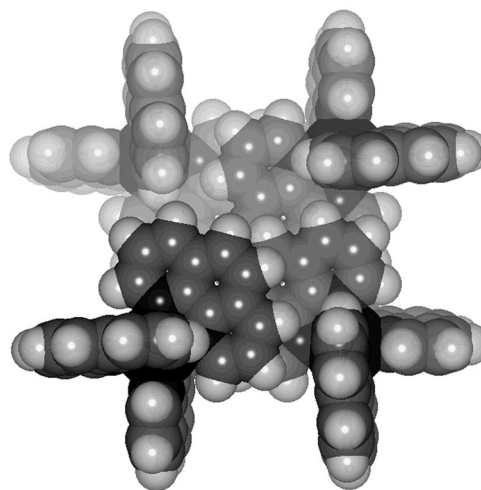


Fig. 21 The fourfold OFF helix of Λ - $[\text{Ru}(\text{phen})_3]^{2+}$ complexes in RAVJIH. Each phen ligand perpendicular to the helix axis forms OFF stack motifs with phen ligands from adjacent molecules in the helix. Each phen ligand parallel to the helix axis (*i.e.* two ligands per complex) receives an EF interaction from an OFF stacked phen ligand of an adjacent complex in the helix.

not crystallise with the motifs described above. There are five reports in the CSD of similar compounds where the crystal structure contains only one enantiomer. One such compound is Λ - $[\text{Ru}(\text{phen})_3][\text{PF}_6]_2 \cdot \text{CH}_3\text{CN} \cdot \text{EtOEt}$ [RAVJIH] which crystallises in the tetragonal space group $P4_3$, with two cations in the asymmetric unit. Each independent cation forms a helical arrangement constructed with OFF and EF local motifs, as illustrated in Fig. 21. This compact and intimate fourfold helical chain of Λ - $[\text{Ru}(\text{phen})_3]^{2+}$ complexes comprises a central OFF stack along the helix axis, using both faces of one phen ligand from each complex. The other two phen ligands are parallel to the helix axis, and each receives one EF interaction from the stacked phen of the adjacent complex. Thus the phen ligands are in two sets, normal and parallel to the helix axis. Those normal to the helix axis are involved in two OFF and one EF interaction, while the phen ligands parallel to the helix axis are involved in one EF interaction. The motif between adjacent pairs of $\text{M}(\text{phen})_3$ complexes in the helix is similar to the homochiral P4AE (Fig. 4(b)).²²

Discussion, conclusions, and predictions

In the progression from observing crystal structure to understanding crystal packing, leading to the design and engineering of crystals, there is a series of basic questions that need response. The principal findings and the significance of the analysis of crystal supramolecularity for M -phen complexes reported in this paper are presented in terms of these questions and responses.

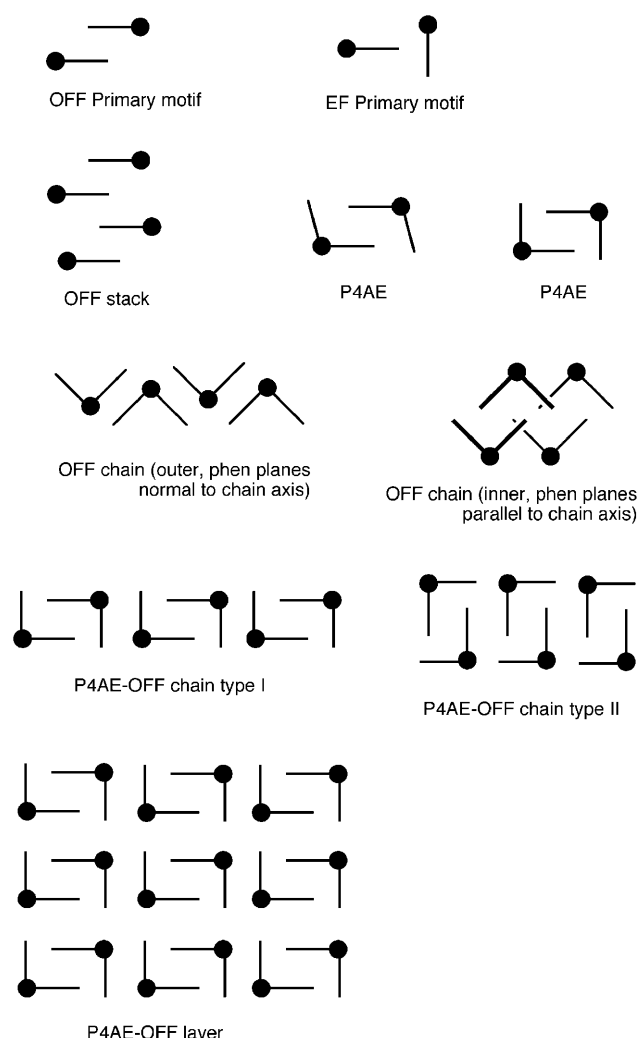


Fig. 22 Diagrammatic representation of the embraces engaged by $M(\text{phen})_n$ complexes. The dot is M, and the lines are phen ligand planes.

1. What are the main local intermolecular motifs for M -phen complexes? The large aromatic surface and extended edge of the phen ligand render it suitable to participate in OFF and EF interactions, with prevalence for the OFF which is present in over 70% of $M(\text{phen})_n$ crystal structures. The EF interaction occurs in only about 13% of $M(\text{phen})_n$ crystal structures, and is frequently accompanied by an OFF in the formation of a P4AE.

2. What are the principal embrace types for M -phen complexes? These are represented diagrammatically in Fig. 22. The preponderance of OFF and P4AE motifs is evident.

3. What are the main crystal supramolecular motifs for complexes only partially coordinated by phen ligands? Nearly 30% of $M(\text{phen})$ compounds crystallise so that they incorporate an OFF stack, conveniently utilising both surfaces of the phen ligand in the formation of interactions which are energetically favourable. For $M(\text{phen})_2$ compounds the prevalent motif is the OFF chain.

4. What are the prevalent crystal supramolecular motifs for $M(\text{phen})_3$ complexes? P4AE chains and OFF chains each occur with about 30% frequency. The 6AE and the $(6\text{AE})_\infty$ chain are rare.

5. What are the intermolecular energies for M -phen complexes? An OFF between two phen ligands can contribute up to 10 kcal mol⁻¹ attraction per $(\text{phen})_2$. The P4AE between two $[M(\text{phen})_3]^{2+}$ cations can contribute up to 9 kcal mol⁻¹ attraction per $\{[M(\text{phen})_3]^{2+}\}_2$.

6. How do the crystal supramolecular motifs of M -phen complexes compare with those of M -bipy complexes? The

proportion of $M(\text{bipy})$ crystal structures containing OFF stacks (25%) is less than that for $M(\text{phen})$ compounds. $M(\text{bipy})_3$ compounds commonly crystallise with the 6AE and the $(6\text{AE})_\infty$ chain, based on EF motifs only, but these are rare for $M(\text{phen})_3$. The differences are consistent with the smaller aromatic ligand area of bipy. The van der Waals attraction in a 6AE interaction for two $M(\text{bipy})_3$ moieties is about 14 kcal mol⁻¹, which is diminished by the net electrostatic energy which ranges from 0 to 25 kcal mol⁻¹ repulsion, depending on the total charge ($z=0, 2+$ or $3+$) on $[M(\text{bipy})_3]^{2+}$. For the case of dipositive $[M(\text{bipy})_3]^{2+}$, comparable with the dipositive $[M(\text{phen})_3]^{2+}$ investigated here, the net energy of the 6AE was calculated to be *ca.* 0.¹² Thus the P4AE for $[M(\text{phen})_3]^{2+}$, with *ca.* 9 kcal mol⁻¹ attraction, is calculated to be a stronger embrace than the 6AE for $[M(\text{bipy})_3]^{2+}$.

7. What are the implications for chiral recognition in crystals? The prevalent P4AE is normally heterochiral (and often exactly enantiomeric), but one instance of a homo-chiral P4AE has been recognised. There is still insufficient information about potentially enantioselective embraces between $[M(\text{phen})_3]$ complexes and other molecules.

The foregoing focuses on crystal supramolecular motifs, but in view of the objectives in crystal design and engineering, understanding of full crystal packing is required, raising further questions.

8. Are there recognisable patterns of crystal packing for M -phen complexes? A number of crystals show dominant slab structures, with well developed and tight embraces between phen ligands within the slab. This occurs for $M(\text{phen})_2$ and $M(\text{phen})_3$ complexes. The orthogonal geometrical character of the ligands in these complexes and of the P4AE and OFF motifs favour this tight packing in slabs. The slab is clearly a hydrophobic domain, and anions and any hydrogen bonding components form hydrophilic domains between the hydrophobic slabs. The influence of this hydrophobic/hydrophilic segregation is evident in the placement of the alkyl and hydroxy functions of ethanol relative to the slab in **1**.

9. What can be predicted about the crystal supramolecularity of M -phen complexes? OFF and P4AE motifs, and their extensions, are likely to occur in $M(\text{phen})_n$ complexes for $n = 1, 2$ or 3 . $M(\text{phen})_2$ and $M(\text{phen})_3$ complexes are likely to have hydrophobic domains constructed from these motifs, and strongly hydrogen bonding components of crystals will be favourably segregated. The hydrophobic domain is likely to be layered, although further analysis is required to understand the crystal packing of $M(\text{phen})_2$ and $M(\text{phen})_3$ complexes with large and shape-awkward anions.

Finally, in the context of crystal design and applications of these principles, we note the reported enantioselective interactions of the tris(tetrachlorocatecholato)phosphate anion with $[M(\text{phen})_3]^{2+}$ (and $[M(\text{bipy})_3]^{2+}$) complexes and derivatives in solution.^{36,37} The crystal supramolecularity of these associations, not yet known, will also guide diastereomeric aspects of crystal engineering.

Acknowledgements

This research is supported by the Australian Research Council. Vanessa Russell acknowledges an Australian Postgraduate Award.

References

- I. G. Dance and M. L. Scudder, *J. Chem. Soc., Chem. Commun.*, 1995, 1039.
- I. Dance and M. Scudder, *J. Chem. Soc., Dalton Trans.*, 1996, 3755.
- I. Dance and M. Scudder, *Chem. Eur. J.*, 1996, **2**, 481.
- C. Hasselgren, P. A. W. Dean, M. L. Scudder, D. C. Craig and I. G. Dance, *J. Chem. Soc., Dalton Trans.*, 1997, 2019.
- M. Scudder and I. Dance, *J. Chem. Soc., Dalton Trans.*, 1998, 329.

- 6 I. Dance and M. Scudder, *New J. Chem.*, 1998, 481.
- 7 M. Scudder and I. Dance, *J. Chem. Soc., Dalton Trans.*, 1998, 3167.
- 8 M. Scudder and I. Dance, *J. Chem. Soc., Dalton Trans.*, 1998, 3155.
- 9 I. G. Dance and M. L. Scudder, *J. Chem. Soc., Dalton Trans.*, 2000, 1579.
- 10 I. G. Dance and M. L. Scudder, *J. Chem. Soc., Dalton Trans.*, 2000, 1587.
- 11 I. G. Dance, in *The Crystal as a Supramolecular Entity*, ed. G. R. Desiraju, John Wiley, New York, 1996, pp. 137–233.
- 12 I. Dance and M. Scudder, *J. Chem. Soc., Dalton Trans.*, 1998, 1341.
- 13 M. L. Scudder, H. A. Goodwin and I. G. Dance, *New J. Chem.*, 1999, 23, 695.
- 14 N. W. Alcock, P. R. Barker, J. M. Haider, M. J. Hannon, C. L. Painting, Z. Pikramenou, E. W. Plummer, K. Rissanen and P. Saarenketo, *J. Chem. Soc., Dalton Trans.*, 2000, 1447.
- 15 F. H. Allen, J. E. Davies, J. J. Galloy, O. Johnson, O. Kennard, C. F. Macrae and D. G. Watson, *Chem. Inf. Comput. Sci.*, 1991, 31, 204.
- 16 F. H. Allen and O. Kennard, *Chem. Des. Autom. News*, 1993, 8, 131.
- 17 A. K. Rappe and W. A. Goddard, *J. Phys. Chem.*, 1991, 95, 3358.
- 18 Cerius 2, MSI, <http://www.msi.com>, 1998.
- 19 *International Tables for X-Ray Crystallography*, eds J. A. Ibers and W. C. Hamilton, Kynoch Press, Birmingham, 1974, vol. 4.
- 20 SIR 92, A. Altomare, M. C. Burla, M. Camalli, G. Cascarano, C. Giacovazzo, A. Guagliardi and G. Polidori, *J. Appl. Crystallogr.*, 1994, 27, 435.
- 21 A. D. Rae, RAELS 92, a Comprehensive Constrained Least Squares Refinement Program, Australian National University, Canberra, 1992.
- 22 C. Horn, I. G. Dance and M. L. Scudder, *CrystEngComm.*, 2001, 1.
- 23 C. Horn, B. F. Ali, I. G. Dance, M. L. Scudder and D. C. Craig, *CrystEngComm*, 2000, 2.
- 24 D. Ramalakshmi, K. R. N. Reddy, D. Padmavathy, M. V. Rajasekharan, N. Arulsamy and D. J. Hodgson, *Inorg. Chim. Acta*, 1999, 284, 158.
- 25 C. Horn and I. G. Dance, 2001, in preparation.
- 26 E. König, G. Ritter and S. K. Kulshreshtha, *Chem. Rev.*, 1985, 85, 219.
- 27 E. König, *Prog. Inorg. Chem.*, 1987, 35, 527.
- 28 H. Romstedt, A. Hauser and H. Spiering, *J. Phys. Chem. Solids*, 1998, 59, 265.
- 29 S. Schenker, A. Hauser, W. Wang and I. Y. Chan, *Chem. Phys. Lett.*, 1998, 297, 281.
- 30 J. A. Real, in *Transition metals in supramolecular chemistry*, ed. J. P. Sauvage, Wiley, New York, 1999, pp. 53–91.
- 31 C. Horn, I. G. Dance and D. C. Craig, 2001, in preparation.
- 32 G. R. Desiraju and A. Gavezzotti, *Acta Crystallogr., Sect. B*, 1989, 45, 473.
- 33 C. Horn, M. L. Scudder and I. G. Dance, *CrystEngComm*, 2000, 9, 1.
- 34 V. M. Russell, D. C. Craig, M. L. Scudder and I. G. Dance, 2001, submitted.
- 35 M. L. Scudder and I. G. Dance, 2001, in preparation.
- 36 J. Lacour, S. Torche-Haldimann, J. J. Jodry, C. Ginglinger and F. Favarger, *Chem. Commun.*, 1998, 1733.
- 37 J. Lacour, C. Goujon-Ginglinger, S. Torche-Haldimann and J. J. Jodry, *Angew. Chem., Int. Ed.*, 2000, 39, 3695.